STUDY OF EXTRUSION OF POLYSTYRENE NANOCOMPOSITE FOAMS WITH SUPERCRITICAL CARBON DIOXIDE

Senior Honors Thesis

by

Shah, Jay

Date: 08/18/05

Table of Contents:

Abstract:

The cell density (bubbles/cm^3 of polymer) and bubble size of the intercalated polystyrene nano-clay composite foams are reviewed as a function of concentration and temperature. 5% intercalated polystyrene nano-clay composites were mixed with pure polystyrene and diluted to prepare 3%, 1%, 0.3%, 0.1% and 0.03% intercalated polystyrene nano-clay composites by mechanical blending with a screw rotation speed of 150 RPM and a temperature of 200° C. Once these nano-clay composites were prepared, they were foamed with supercritical carbon dioxide as the foaming agent in a batch foaming process at the temperatures of 80° C, 100° C and 120° C. Different concentrations of these intercalated polystyrene nano-clay composite foams were compared with the pure polystyrene foam at 120° C. Also, 3% intercalated polystyrene nano-clay composite foam at 80° C, 100° C and 120° C were compared. The number of bubbles/cm^3 of polymer increased and the bubble size decreased with the increase in concentration of the intercalated polystyrene nano-clay composite foams, other conditions being constant, although the pure polymer was found to have the maximum cell density and the least bubble size. The cell density decreased and the bubble size increased with the increase in temperature at which the intercalated polystyrene nano-clay composite was foamed. Only three samples were used in examining the effect of temperature and there was inconsistency in the results obtained. Hence, a convincing conclusion for the relation between the temperature at which the polymer nanocomposite was foamed and the cell density as well as the bubble size was not obtained.

Introduction:

The last decade has seen extensive research on microcellular and nanocellular polymeric foams due to the wide variety of applications of foams depending on the type of cells present in the foamed samples. If the foamed samples have cells that are interconnected they are called open cell foams. This type of foam could be used for applications in tissue engineering, chemical engineering purification processes like filtration and separation, other day to day processes such as absorption, insulation, etc. The polymeric foams could also have cells that are not interconnected. Due to their light weight and non-permeable nature this type of foams are called closed cell foams and are used in several day to day applications such as high impact protective clothing, medical equipments, gaskets, cushions, plastic bottles, films, etc. Figure 1 below explains the use of polymeric foams.

(a) (b) (c)

Figure 1: Pictures showing applications of polymeric foams in different industries; a) automotive parts (closed cell); b) internal printer components (closed cell); c) sponge rubber (open cell)

This research project was mainly about preparing intercalated polystyrene nano-composite foams and reviewing the effect of the concentration of these foams on the cell density and bubble size as well as the effect of temperature at which these foams were made on the cell density and the bubble size. The nanocomposites are made up of pure polymer and nanofilter particles. Addition of a small quantity of these nanofilter particles changes physical properties such as barrier resistance, flame retardance, thermal stability, mechanical strength, etc of the polymer particles substantially. Materials that improve the surface aspect ratio and surface area are of particular interest such as smectite clays like montmorillonite which are hydrophilic and help in homogenous dispersion in organic polymer phase, (4). Materials that reduce the surface energy are also significant as they help in improving the wetting characteristics of the clay. Structurally two forms of polystyrene and clay nanocomposites are possible namely, intercalated and exfoliated. Penetration of polymer chains into the interlayer region and interlayer expansion gives rise to intercalated nanocomposite. Usually the ordered layer structure of the clay is preserved and can be detected by wide angle X-ray diffraction (WXRD). On the other hand, extensive polymer penetration, silicate crystallites delamination and dispersion of individual nanometer thick platelets in the polymer matrix gives rise to exfoliated nanocomposite that usually provide a large aspect ratio and surface area. Polymer nanocomposites are usually prepared by melt intercalation or in-situ polymerization, (4).

Once these polymer nanocomposites are synthesized, they can be foamed using a foaming agent such as carbon dioxide. The foamed polymeric nanocomposites are used in a wide variety of applications such as insulation, cushion, packaging, automobiles, airline industry, etc. Microcellular foams having cell sizes less than 10 μm and cell

density greater than 10^9 per cm^3 of polymer can reduce the material use without affecting the mechanical properties and by improving the strength, toughness and fatigue life, (5). Although the microcellular foams have a narrow operating range, they exhibit a high strength-weight ratio as compared to common foams. Powders of organic, inorganic or metallic material can control the cell structures of many foamed materials. In the past, many properties along with nucleation of a polymer-gas system have been studied. Microcellular nucleation of bubbles can of either homogenous or heterogeneous. Homogenous nucleation occurs when gas molecules dissolved in a homogeneous polymer come together for a long enough period of time to produce a stable bubble nucleus and the bubbles nucleate homogeneously. Heterogeneous nucleation occurs when a bubble forms at an interface between two phases such as a polymer and an additive, (3). The rate of nucleation is given by

$$N = f \cdot C \cdot \exp(-\Delta G_{het}\,^* / (k \cdot T)) \qquad (1)$$

where N is the rate of heterogeneous nucleation, f is the frequency factor of gas molecules joining the nucleus, C is the concentration of the heterogeneous nucleation sites, k is the Boltzmann's constant, T is the temperature and $\Delta G_{het}\,^*$ is the nucleation energy, which is related to the interfacial tension σ, wetting angle θ at the polymer additive gas interface, (1). The pressure difference ΔP in and out of the cell is found using:

$$\Delta G_{het}\,^* = 16 \cdot \pi \cdot \sigma^3 \cdot f(\theta) / (3 \cdot \Delta P^2) \qquad (2)$$

where $f(\theta)$ is 1 for homogenous nucleation and for heterogeneous nucleation

$$f(\theta) = (1/4) \cdot (2 + \cos\theta) \cdot (1 - \cos\theta)^2 \qquad (3)$$

People have shown before that with increase in saturation pressure, the nucleation rate increases. Also, presence of the soluble additive decreases the intermolecular potential

thus decreasing the activation energy required to nucleate a bubble. Usually heterogeneous nucleation has a lower activation energy barrier than homogeneous nucleation, (3). Due to this, a heterogeneous nucleated bubble will nucleate before a homogenous nucleated bubble and an average heterogeneous bubble will be bigger than an average homogeneous bubble. Comparing to the conventional micron sized filler particles used in the foaming process, nanometer sized clay particles offer extremely fine dimensions, large surface area and intimate contact between particles and polymer matrix. Thus, nano sized particles not only significantly affect the cell nucleation and growth but also provide benefits to the structure and properties of the polymer, (5).

In this work, the 5% intercalated polystyrene nano-clay composites were obtained and diluted to different concentrations by mixing the composites with pure polystyrene. These composites and pure polystyrene samples were then foamed at different temperatures with supercritical carbon dioxide. Supercritical carbon dioxide is used as a foaming agent due to the several advantages it shows at the supercritical state as compared to traditional foaming agents. At supercritical state, the temperature of carbon dioxide is 31° C and 73.8 bar or 1074 psi. The high diffusivity makes it possible to dissolve sufficient carbon dioxide in a polymer melt quickly. Carbon dioxide can reduce the viscosity and surface tension of polymer melts, which assists in many polymer processing operations. Also, carbon dioxide is low cost, non flammable, environmentally friendly and chemically benign. Tomasko *et al*. review the applications of carbon dioxide in processing of polymers and the future of carbon dioxide in polymer applications, (7). A batch foaming process was used to foam the intercalated polystyrene nanocomposites. After the intercalated polymer nanocomposites are foamed with carbon dioxide, they are

dissected in liquid nitrogen. The cross sections of the polymeric foams are analyzed with the help of the images obtained from a scanning electron microscope (SEM). The cell density and bubble size were determined from the analysis of the images obtained and by using the formulas from the literature. Finally, the variation of the cell density and bubble size with concentration and temperature is reviewed for the intercalated polystyrene nanocomposite foams prepared using supercritical carbon dioxide as the foaming agent.

Literature Review:

After Toyota's work in polymer layered silicate nanocomposites, extensive research has been carried out in this field. Although nucleation mechanism is not well understood, recent research has shown progress in this field. Martini, Suh and Waldman showed that saturated samples may be heated to a temperature higher than the glass transition temperature to produce foams of lower density, (1).The first microcellular foams were produced in high impact polystyrene by Martini *et al*. using nitrogen as the nucleating gas. The majority of work on microcellular foams to date has been conducted on the polystyrene-nitrogen system by Martini *et al*., Waldman, Kumar, Colton and Suh, (2). While studying the effect of talc on cell nucleation of propylene, Park *et al.* found that when isopentane is used to foam propylene, cell nucleation is dominated by talc concentration. Whereas, when CO_2 is used as a foaming agent, cell nucleation is dominated by talc concentration only at low CO_2 content after which CO_2 content determines the cell nucleation. Ramesh *et al.* developed a model for heterogeneous nucleation in blend of polystyrene and high impact polystyrene, (5).

Previous research has also proved that an addition of a small quantity of these nano-sized particles in the polymer significantly improves the physical properties such as strength, thermal stability, flame retardance and barrier resistance. The addition of these particles may also improve cell nucleation and growth. Nam *et al.* investigated the influence of foaming polypropylene clay nanocomposites on cell size, cell density, cell wall thickness, and bulk density. Also, foams with finer fillers show that cell density is directly proportional to the saturation pressure, (5). Chen *et al.* found that more CO_2 was absorbed by filled polymers due to the accumulation of the gas on the filler – polymer

interface, which helps in creating more nucleation sites. Colton *et al*. investigated nucleation theory in polystyrene – zinc stearate system and extended their case from homogenous to heterogeneous nucleation, (5). They explain how heterogeneous nucleation occurs above the solubility limit of the additives and that the concentration affects the number and size of bubbles as well as the structure of the walls. They considered the volume change due to the presence of dissolved gas and surface tension change due to the presence of a third phase, as well as their influence on Gibbs free energy of nucleation. Transmission electron microscopy has proved that biaxial flow during cell growth induces alignment of clay particles along cell periphery.

Polymeric nanocomposite foams not only reduce the cost of the material used, but also provide more efficient products with improved mechanical and physical properties, for example, use of polymeric foams in automobile industry, construction industry, heat exchanging devices, etc. Han *et al*. also showed in their work that the exfoliated polystyrene nanocomposites foamed using supercritical carbon dioxide showed better physical and mechanical properties as well as higher cell density and the smallest cell size, (5). They also showed that combining nanocomposites and the extrusion foaming process provides a new technique for the design and control of cell structure in microcellular foams. Zeng *et al*. manipulated the cell morphology by modifying the interaction between carbon dioxide and clay surface, (4). They studied the dimension stability of nanocomposites and related to both nanoscale and mesoscale clay dispersion. A strong affinity between carbon dioxide and carbonyl group may greatly reduce the gas-particle interfacial tension which reduces the nucleation energy and increases the rate of nucleation. V. Kumar and J. Weller concluded in their description about the process to

produce microcellular PVC that bubble nucleation density increases with foaming temperature and eventually reaches a limiting value, while the average bubble diameter is relatively independent of the foaming temperature, (1). They also concluded that the majority of the cell growth occurred in the early stages of foaming. In their description of the process to produce microcellular polycarbonate using carbon dioxide for bubble nucleation, results on solubility, bubble nucleation and bubble growth in polycarbonate-carbon dioxide systems are presented along with key process parameters, (2). Also, they showed that the bubble nucleation phenomenon in polycarbonate near the glass transition temperature is not described by the classical nucleation theory. Along with that, they concluded that the foam density varied linearly with the foaming temperature and the bubble nucleation density was found to be relatively independent of foaming temperature in the range 60-160° C whereas the bubble size was found to increase with the increase in the foaming temperature. In addition, they derived a relationship between the cell density and average cell diameter with saturation pressure. Nam et al. also derived a relationship between the nucleation rate and the saturation pressure as well as the relationship between the nucleation rate and number of bubbles with weight % of zinc stearate, (3). They concluded that the number of bubbles increases with the concentration of zinc stearate up to the solubility limit. Above the solubility limit heterogeneous nucleation occurs and the number of bubbles is no longer dependent on saturation pressure. Heterogeneous nucleation is energetically favored due to its lower activation energy barrier which helps in dominating the nucleation process. The number of bubbles increases with the increase in the nucleation sites.

Experimental:

Materials/Equipment

5% Intercalated polystyrene nano-clay composites, pure polystyrene, microcompounder with tools and cleaning material, weighing machine, batch foaming setup with proper valves, supercritical carbon dioxide, tool box, stainless steel or aluminum tube with proper screws to close it from both ends, kim wipes, thermocouple, insulation straps or pads, soap water, liquid nitrogen, sharp blade, tongs, pallets, equipment to coat the samples with alloy of gold and platinum, scanning electron microscope (SEM), computer connected to SEM and paper to print the images.

Synthesis of different concentrations of intercalated polystyrene nano-clay composites from 5% samples

The 5% intercalated polystyrene nano-clay particles made available were used to prepare the different concentrations of the intercalated polystyrene nano-clay composites. This was the first step of the experimental. The 5% composites were mixed with pure polystyrene in appropriate quantities to obtain different concentrations of intercalated polystyrene nano-clay composites using a microcompounder and its tools. The microcompounder was operated at the screw rotation speed of 150 RPM and 200° C with a force greater than 90 N. The microcompounder has the capacity of mixing about 5 gram solids at a time. Thus, exact weight of 5% nanocomposite and pure polystyrene was calculated using simple math to obtain the desired concentration of the intercalated polystyrene nano-clay composite. For example, 3 is 60% of 5, and so, to get 3% nanocomposite from 5% nanocomposite, 60% of 5 gram (3 gram) has to be 5%

nanocomposite. This 3 gram of 5% nanocomposite is mixed with 2 gram pure polystyrene particles to get 3% intercalated polystyrene nanocomposite particles. In a similar fashion along with one batch of 3% nanocomposite, two batches of 1% nanocomposite were prepared by mixing 1 gram of 5% nanocomposite along with 4 gram of pure polystyrene. One of the two batches of 1% nanocomposite was used to prepare one batch of 0.3% and two batches of 0.1% nanocomposite. To prepare 0.3% nanocomposite, 1.5 gram of 1% nanocomposite was mixed with 3.5 gram pure polystyrene and to prepare 0.1% nanocomposite, 0.5 gram of 1% nanocomposite was mixed with 4.5 gram of pure polystyrene. 0.03% nanocomposite was then prepared using one of the batches of 0.1% nanocomposite by mixing 1.5 gram of the latter with pure polystyrene. All the different concentrations are not prepared using 5% nanocomposite for better accuracy while using the weighing machine. If 5% nanocomposite is used to prepare 0.01% nanocomposite, it is difficult to weigh the required amount of 5% nanocomposite with accuracy since a very small quantity of 5% nanocomposite would be required as compared to pure polystyrene. This would result in improper mixing and hence 1% and 0.1% are used to make 0.3% and 0.03% respectively to yield better mixing and accuracy in concentration as well as to help weigh the raw material better. It is important to follow the instructions manual while operating the microcompounder to synthesize these nanocomposites and the equipment has to be cleaned after every run by introducing the cleaning material in the microcompounder just like the raw material and right after all the material inside the equipment is collected from the exit. During each run the raw material is entered slowly and mixed for about 5 minutes after all the 5 gram of raw material is inside the microcompounder.

Figure 2: Microcompounder with its plates open

The above figures give information about the microcompounder that was used to synthesize the nanocomposites. Figure 2 shows the microcompounder with its plates open. We can see the rotating screws in this picture very clearly. Figure 3 below shows the microcompounder with its plates closed. This is the way the equipment looks when the material is being mixed in the machine. The big hole near the top of the metal plates at their intersection is where the raw material is introduced from and a small hole near the bottom of the left hand side plate is the exit of the equipment from where the synthesized nanocomposite is collected. The screws on each side of the plates are tightened to ensure

that there is no gap between the plates during the mixing process to avoid wastage of the material.

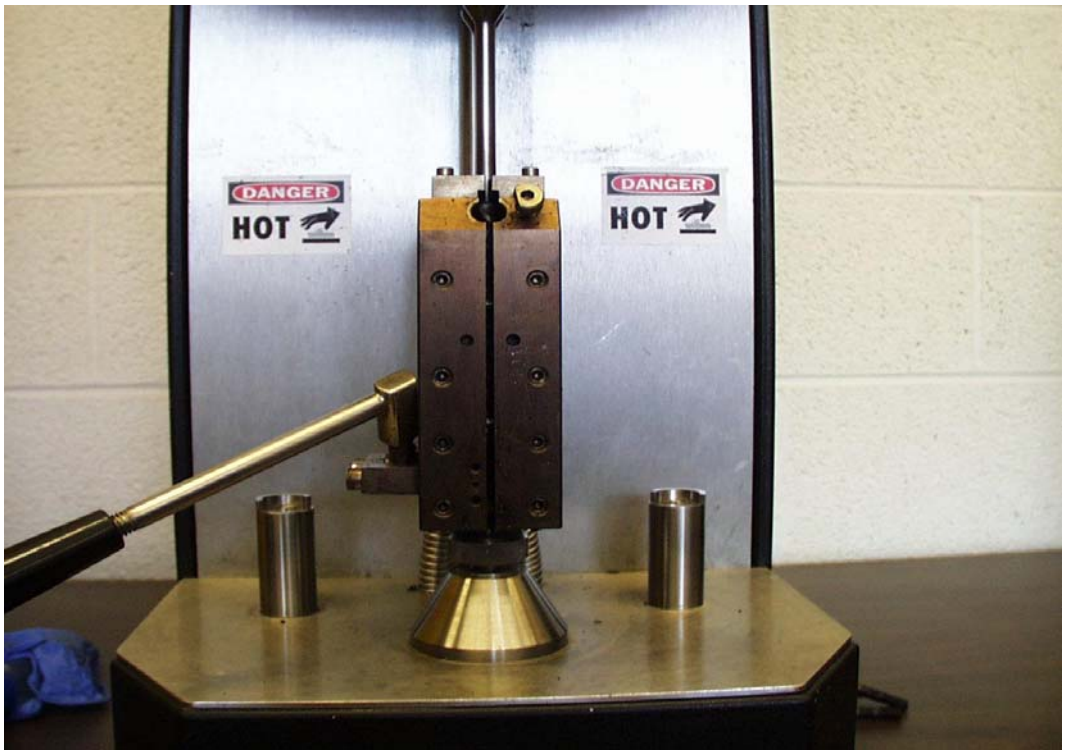

Figure 3: Microcompounder with its plates closed

The operating conditions for the microcompounder are set using the unit placed on top of the microcompounder as shown in figure 4. The heaters are switched on to heat the metal plates at a temperature of 200° C and the screw rotation speed of 150 RPM is set. The screw at the bottom of the plates is rotated so that the force is greater than 90 N after which the rotation between the plates begins. The same conditions are used for all the samples.

Figure 4: Figure showing the top of the microcompounder used to set the operating conditions.

Batch foaming of the intercalated polystyrene nano-clay composites with supercritical carbon dioxide

After obtaining the samples from the microcompounder, a small cylindrical portion of each of these samples is foamed using supercritical carbon dioxide in a batch foaming process. The batch foaming is carried out at three different temperatures for each sample. The three temperatures at which the trials were performed are 80° C, 100° C and 120° C. Three samples of different concentrations were loaded at once in a stainless steel/aluminum tube closed with the help of rotating screws on both ends. These samples

were separated into the tube with the help of kim wipes and the samples were supported against the walls of the tubes. The screws at both ends of the tubes were tightly closed to make sure there is no leakage of carbon dioxide after the samples are loaded and the tube is attached to the setup. Figure 5 below shows the batch foaming setup used to foam the polystyrene nano-clay composites with supercritical carbon dioxide.

Figure 5: Batch foaming setup showing the pump used in the process (the one on the left hand side in the figure) which was connected to the carbon dioxide tank maintained under supercritical conditions.

Once the samples are loaded in the tube after refilling the pump with carbon dioxide and the tube is connected to the above shown set up, all the connections are made tight to avoid carbon dioxide leakage and after this the pump is ran. The valve on the left hand side attached to the pump is then gradually opened to raise the pressure to about 2000 psi. After this, the soap water bubbles are used to determine the leakage of carbon dioxide at all joints and connections in the system. The trial is stopped if a leak is observed. All the connections are tightened again and the procedure is repeated. Once we make sure that there is no leakage of carbon dioxide, the thermocouple is introduced in the system by attaching it to the outside wall of the tube in which the samples are loaded. This tube is covered with insulation straps and/or pads to keep the temperature constant. The setup is observed every half hour for about three hours for stability in numbers and after about 18-20 hours the run is stopped and the foam is obtained from the tube. While stopping the run, the valve attached to the pump on its left hand side in figure 4 is closed slowly to stop the carbon dioxide flow. This is followed by a quick opening of the vent valve located on the left hand side of the pump and next to the valve attached to the pump, to vent out the carbon dioxide. After the carbon dioxide is vented out and the pressure is released, the foaming is complete. The tube was allowed to cool after this for a period of about 15-20 minutes before the samples were collected. In this manner, all the samples were foamed and cross sections of the foamed samples were then analyzed using a scanning electron microscope (SEM) for cell density and bubble size.

Obtaining images of cross sections using a scanning electron microscope (SEM) for analysis

The samples were dissected by introducing them into liquid nitrogen and then breaking them with the help of tongs. To ease the breaking of the samples, a small cut can be made in the sample using a sharp blade. These cross sections were then mounted on pallets which are then coated with an alloy of gold and platinum. These coated samples were loaded in the scanning electron microscope which is connected to a computer. With the help of this computer several images of the cross section were captured at different places along the cross sections with varying magnifications to compare and analyze the cell density and bubble size as well as the uniformity in foaming and several other characteristics of the foamed samples. Only the 3%, 0.3%, 0.03% and pure polymer samples at 120° C were used to review the effect of concentration on the cell density and bubble size. 3% samples at 80° C and 100° C were used along with 3% sample at 120° C for analysis of the effect of foaming temperature on the cell density and bubble size. Due to shortage of time only six samples and two parameters were reviewed in this work.

Results and Discussion:

Analyzing the scanning electron micrographs of the foamed nanocomposite samples to review the effect of varying concentration and temperature

After obtaining all the images of the selected concentrations at varying magnifications and at different locations along the cross section, these images were analyzed for the cell density and the bubble size and their relation with the concentration and foaming temperature was reviewed. Images with a magnification of 500x were selected for the analysis purposes. A scale was used to draw a box on the image and the number of cells present in the box was noted down. If an entire bubble was not included inside the walls of the box drawn then the bubble would be taken into consideration if more than half the bubble was assumed to be inside the boundary of the drawn box. This was done for all the samples and the number of cells present in the boxes drawn was determined. The area of the box drawn was also noted.

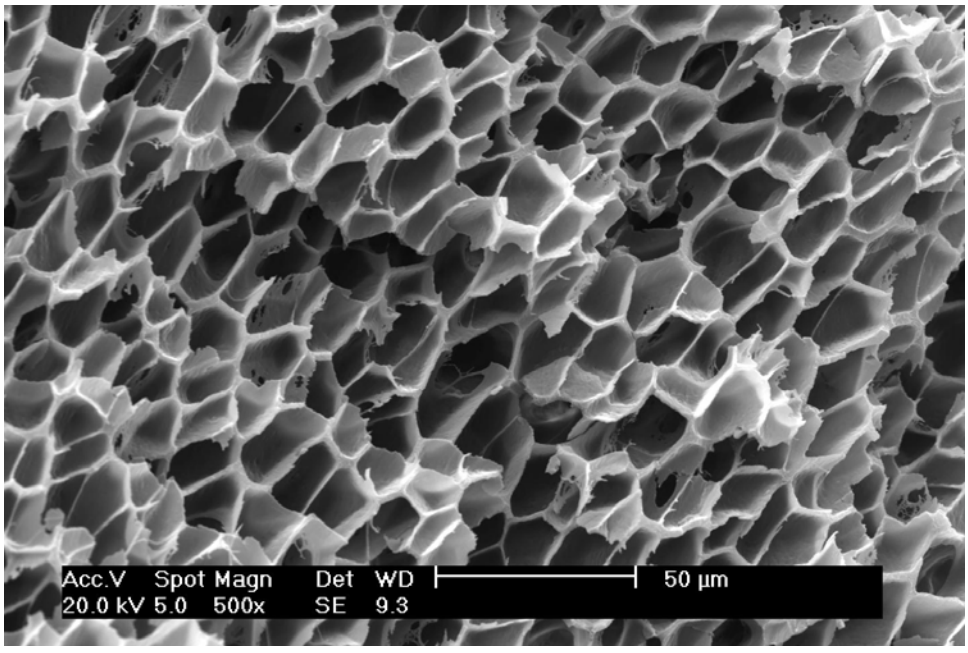

(a)

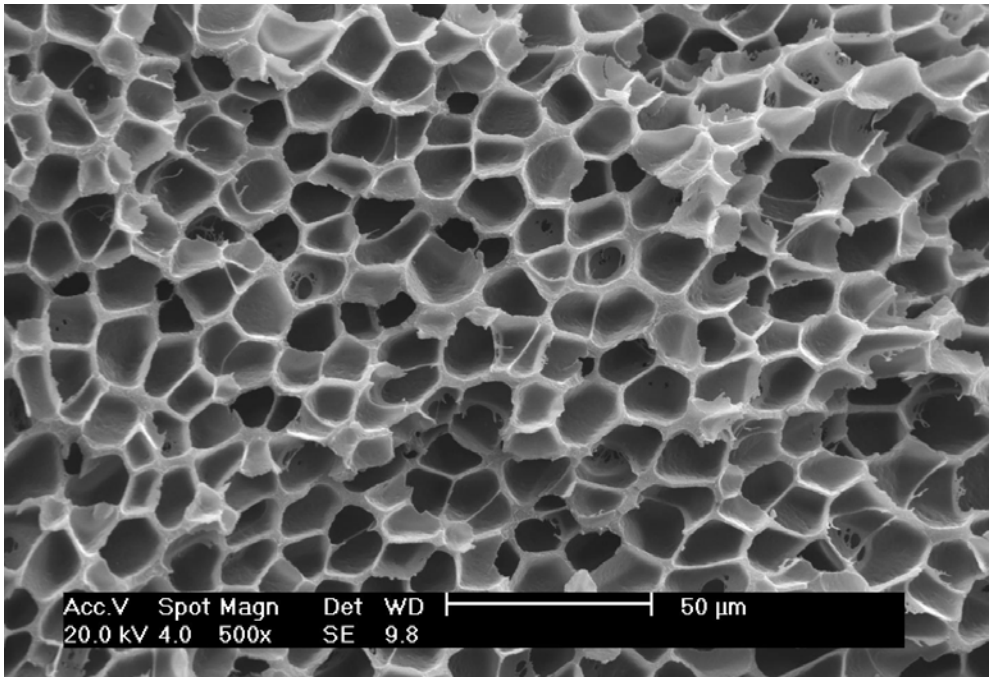
Acc.V Spot Magn Det WD 50 µm
20.0 kV 4.0 500x SE 9.8

(b)

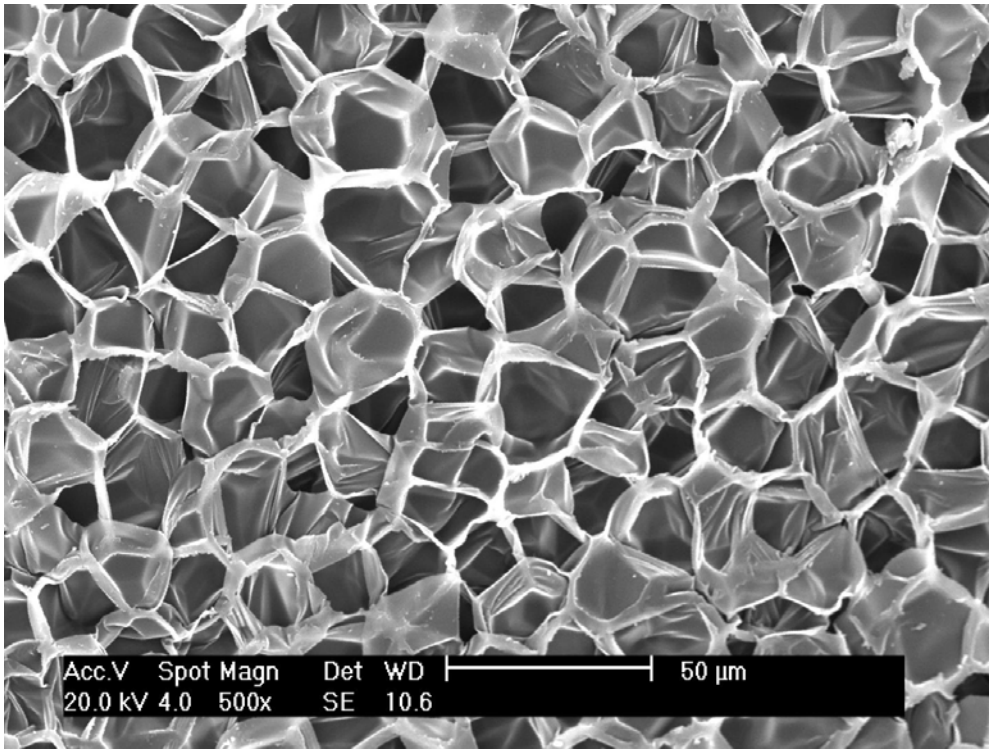
Acc.V Spot Magn Det WD 50 µm
20.0 kV 4.0 500x SE 10.6

(c)

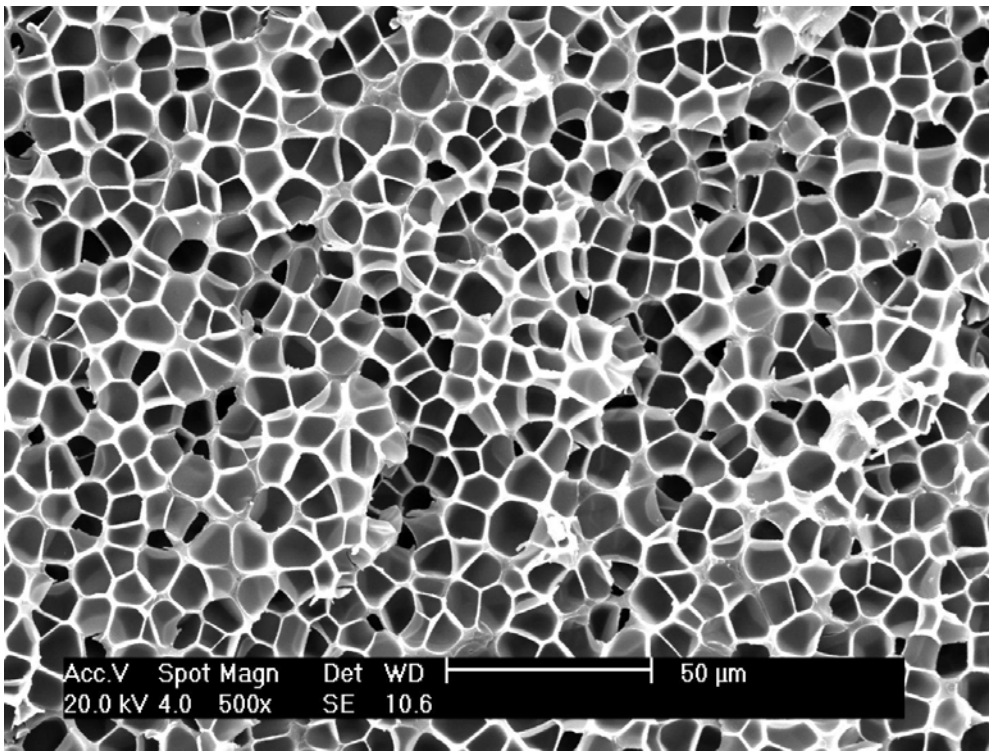

(d)

Figure 6: Scanning electron micrographs at 120° C; (a) 3%; (b) 0.3%; (c) 0.03%; (d) Pure polystyrene

The above figures show the scanning electron micrographs at 120° C for 3%, 0.3%, 0.03% and pure polystyrene with a magnification of 500x. There is a noticeable difference between each one of them as far as the number of bubbles and cell size are concerned. The bubbles become more spherical looking as the concentration decreases. Also the cell walls seemed to become thin as the concentration decreases. In the 3% case, the cells are elongated. This could be possible if the cross section is near the boundary of the sample or if the sample did not enough room to expand horizontally during foaming in the tube. This could result in vertical expansion which could elongate the bubbles.

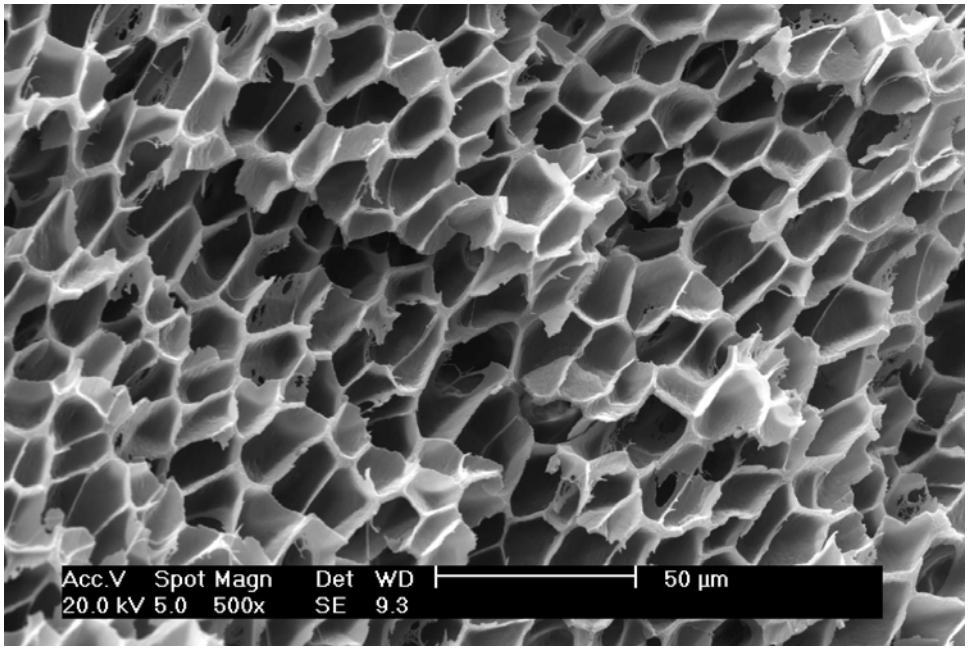
Acc.V Spot Magn Det WD 50 µm
20.0 kV 5.0 500x SE 9.3

(a)

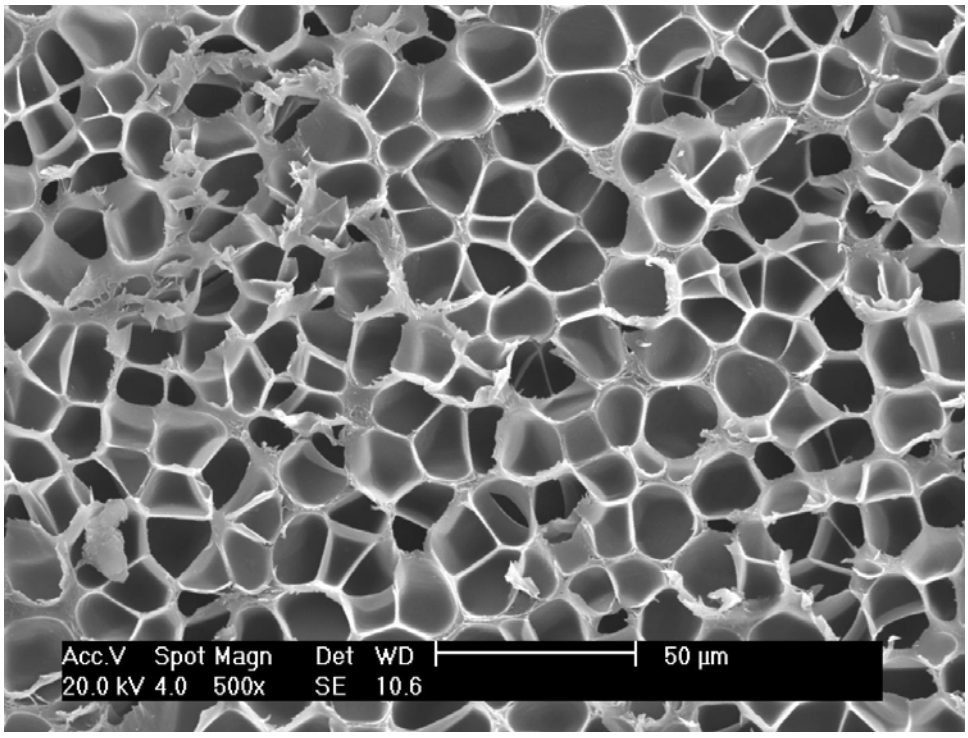
Acc.V Spot Magn Det WD 50 µm
20.0 kV 4.0 500x SE 10.6

(b)

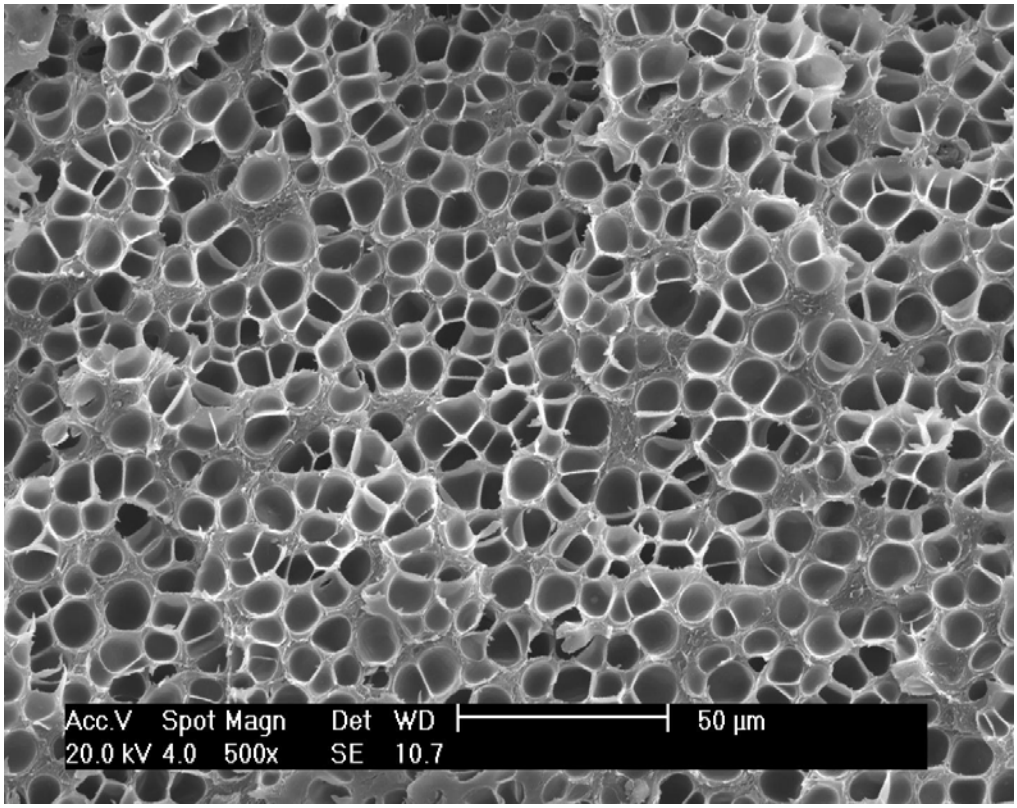

(c)

Figure 7: Scanning electron micrographs of 3% intercalated polystyrene nanocomposites at different temperatures; (a) 120° C; (b) 100° C; (c) 80° C.

The above three figures show scanning electron micrographs for 3% intercalated polystyrene nanocomposite at different temperatures of 120° C , 100° C and 80° C . The difference in the number and the size of the bubbles is very evident as temperatures vary from the above pictures. The cell walls appear to thicker as the temperature decreases and cells look more spherical as the temperature decreases. For all the images in figure 6 and 7, number of cells in a fixed area and the area (cm^2) was noted in a similar fashion. Also, the bubble sizes were found by averaging the diameters of 25-50 bubbles in the

micrograph. After obtaining the magnification factor, number of cells within the box drawn and the area of the box drawn on the micrographs, the cell density of the foam was determined by using

$$N_f = (n \cdot M^2 / A)^{3/2} \quad (4)$$

where N_f = the number of cells per cm^3 of foam, n = number of cells in the micrograph, M = magnification of the micrograph, A = area of the micrograph (cm^2).

The above formula is based on the assumption that the cell distribution in the foam is homogeneous and isotropic. The area cell density is defined as number of cells, n, divided by the actual area which is A/M^2 and the line cell density is the square root of the area cell density. Thus, the number of cells nucleated per unit volume of foam is obtained by cubing the line cell density. The number of cells nucleated per unit volume of the original polymer is called the cell density which is determined by dividing the number of cells per unit volume of foam by the volume of polymer in a unit volume of foam. The volume of polymer per cm^3 of foam is $(1-V_f)$, where V_f is the void fraction of the foam. The void fraction, or volume occupied by the voids per cm^3 of foam can be estimated by multiplying the volume of an average cell by the number of cells per cm^3 of foam. The average diameter, D, of a cell in the micrograph is obtained by averaging the diameters of 25-50 bubbles in a SEM micrograph and scaling them appropriately based on the scale provided on the SEM micrograph (2.6 cm = 50 μm). Once N_f and D are known, the void fraction can be calculated using

$$V_f = \pi \cdot D^3 \cdot N_f / 6 \quad (5)$$

Once the void fraction of the foam is obtained, it is used along with the number of cells per unit volume of foam to find the number of cells nucleated per unit volume of original polymer, N0, which is given by

$$N_0 = N_f /(1 - V_f) \qquad (6)$$

The cell density reported is given by equation (6), (1).

Effect of varying concentration on cell density and the bubble size at constant temperature

After analyzing the scanning electron micrographs and using the above mentioned equations, the cell density and the bubble size of the foamed samples for varying concentration at a constant temperature was determined. These results are tabulated in table 1 shown below.

Table 1: Table showing the cell density and bubble size for different concentrations at 120° C

Concentration (%)	Temperature (° C)	No. of bubbles per cm^3 of foam x 10^{-8} (N_f)	Bubble size (μm)	Void fraction of foam	No. of bubbles per cm^3 of polymer x 10^{-9} (N_0)
3	120	6.84	12.98	0.78	3.15
0.3	120	2.59	17.98	0.79	1.22
0.03	120	1.61	19.33	0.61	0.41
Pure Polystyrene	120	18	8.37	0.55	4.02

After obtaining the above data, the cell density and the bubble size information was used to plot graphs of the variation of cell density and bubble size versus varying

concentration. Figure 8 below shows the changing cell density with varying concentration.

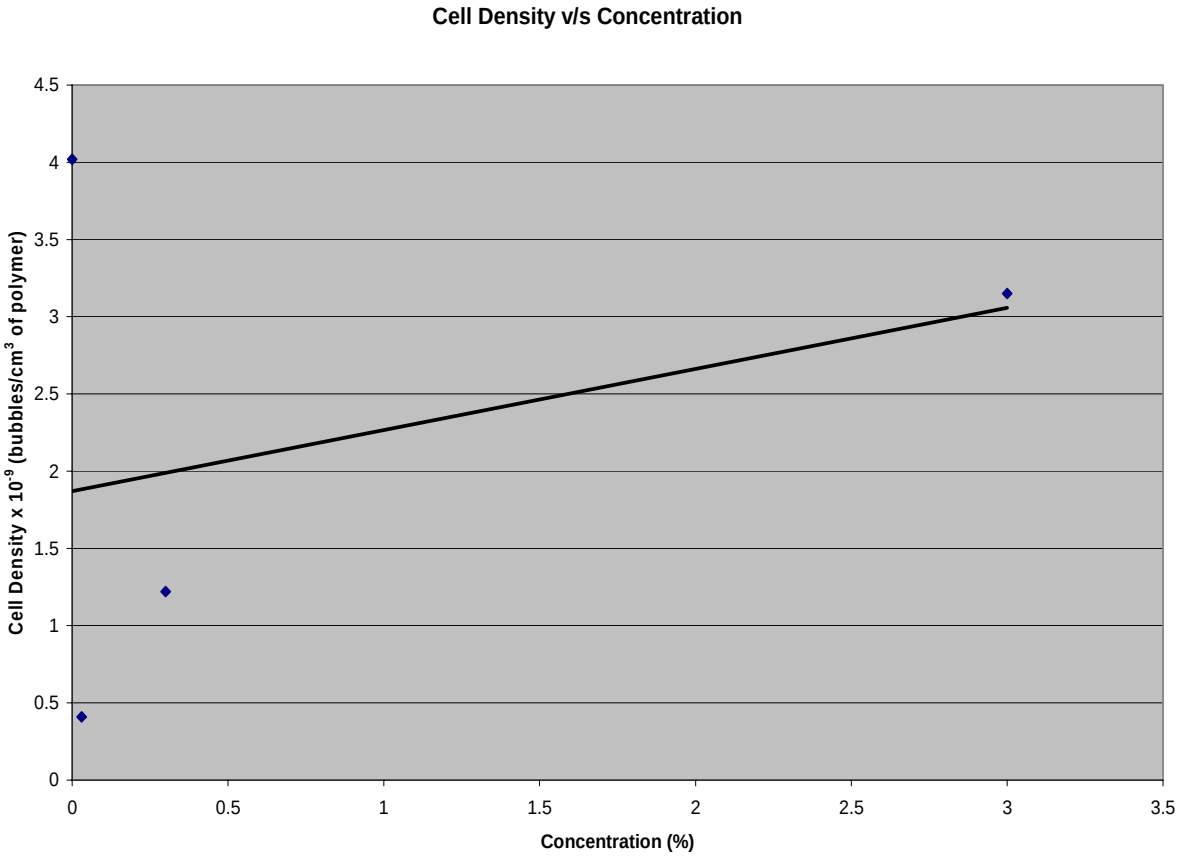

Figure 8: Plot showing variation of cell density with varying concentration at 120° C.

From the above plot we can say that the cell density increases as the concentration of the foamed polystyrene nanocomposites increases. Thus, larger the amount of the additive clay particles, higher is the cell density. More additive particles cause more nucleation sites and hence increase the rate of nucleation and the number of cells thus increasing the cell density. Reduction in the surface energy due to the increasing concentration of clay in polystyrene reduces the activation energy barrier to nucleation. The only exception was the case of pure polymer. The 3%, 0.3% and 0.03% were foamed

during the same trial in the same tube. The pure polymer was foamed at the same temperature along with 1% and 0.1% in a different run at a different time. This could be the only possible reason why the result of pure polymer is inconsistent with the rest of the data. Experimental error could have resulted in such inconsistency. Overall, the trend of increasing cell density with increasing concentration is in agreement with literature. Nam *et al*. concluded that the cell density increases as the concentration of the additive increases, (3). The additive they used was zinc stearate. In both the cases the nucleation is assumed to be homogeneous.

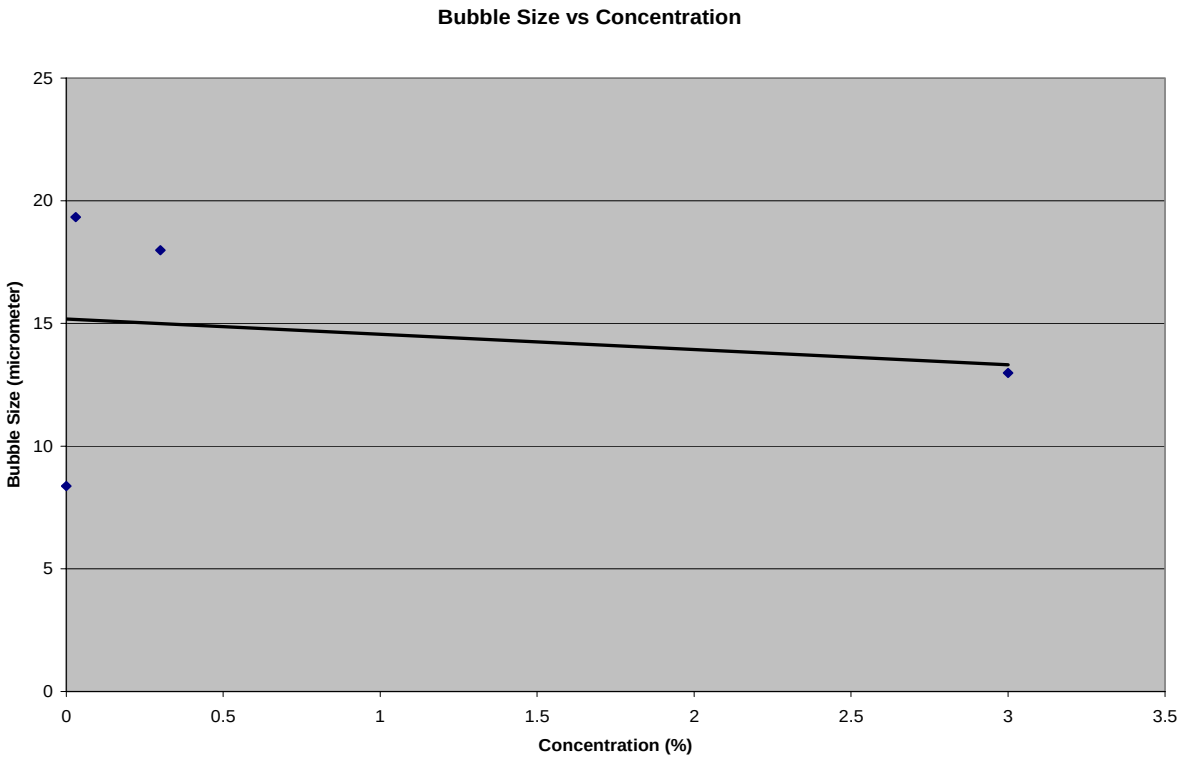

Figure 9: Plot showing the variation of bubble size with varying concentration at 120° C.

The graph above shows the variation of the bubble size with the varying concentration at 120° C. From the above graph we can conclude that the bubble size

decreases with the increasing concentration at a constant temperature. Again the pure polymer case was an exception probably due to some experimental error. The pure polystyrene was expected to have the highest bubble size and the least cell density but it ended up having the least bubble size and highest cell density. Increasing concentration of clay in polystyrene gives rise to more nucleation sites causing more bubbles and smaller bubbles to form. This strengthens the polymer and improves the physical and the mechanical properties of the polymer as well as helps in reducing the use of polystyrene.

Effect of varying temperature on cell density and the bubble size with constant concentration

After analyzing the scanning electron micrographs and to determine the cell density and the bubble size of the foamed samples for varying concentration at a constant temperature, the same set of calculations were performed for 3% intercalated polystyrene nanocomposites at different temperatures using the same set of equations. The results obtained for cell density and bubble size at varying temperatures of these nanocomposites are tabulated below in table 2.

Table 2: Table showing bubble size and cell density for 3% intercalated polystyrene nanocomposites at varying temperatures

Concentration (%)	Temperature (° C)	No. of bubbles per cm^3 of foam x 10^{-8} (N_f)	Bubble size (μm)	Void fraction of foam	No. of bubbles per cm^3 of polymer x 10^{-9} (N_0)
3	120	6.84	12.98	0.78	3.15
3	100	4.35	14.52	0.70	1.45
3	80	20.76	8.32	0.63	5.61

Using the data obtained from the above table regarding the change in cell density and bubble size with varying temperature conditions, plots of cell density and bubble size versus temperature are generated to review the relationship between the foaming temperature and cell density as well as bubble size. Figure 10 below shows the variation of cell density with change in temperature.

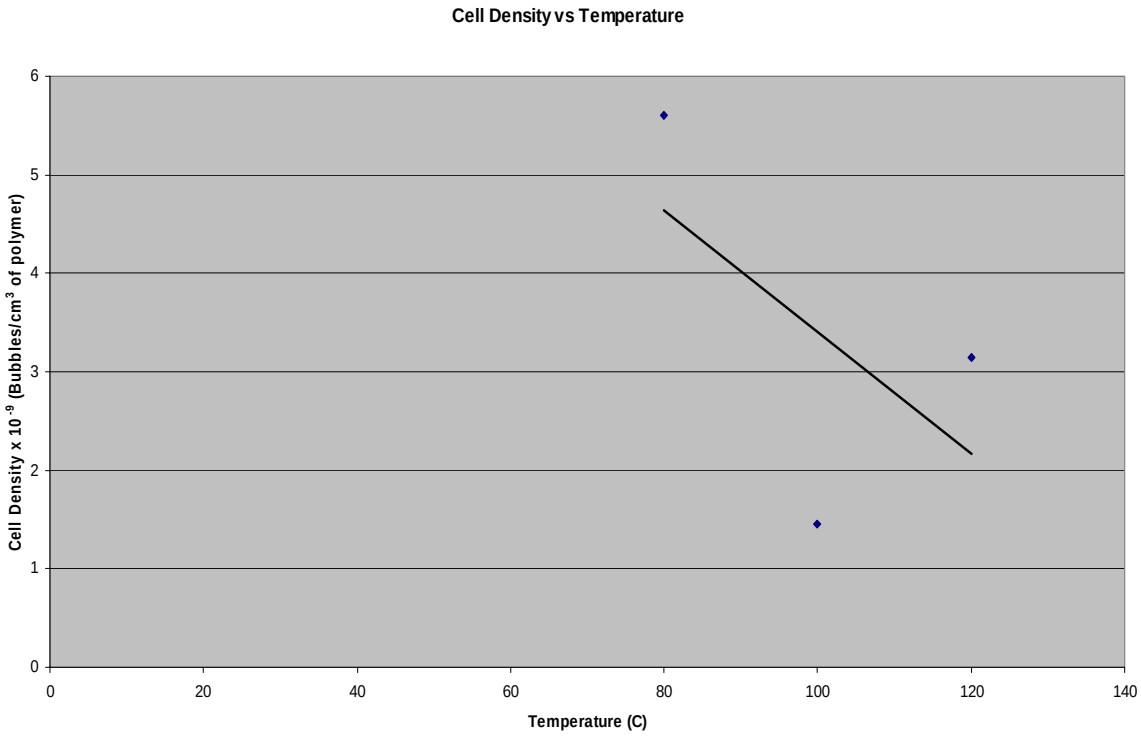

Figure 10: Plot showing the variation of cell density with varying temperature for 3% nanocomposite foams

From the above plot we cannot really define a relation between the foaming temperature and cell density although a linear trend line shows that the cell density decreases with increasing foaming temperature. Many other parameters such as solubility of carbon dioxide in the polymer, viscosity of the polymer, surface tension, surface energy,

nucleation energy, foaming time, saturation pressure, etc. determine the cell density along with foaming temperature and concentration. With change in temperature, some of these properties change too and hence it is difficult to predict the behavior of cell density with varying temperature with only three data points. Since cell density is very sensitive to change in foaming temperature, atleast 8-10 points would be required to review and derive a more convincing relationship between foaming temperature and cell density.

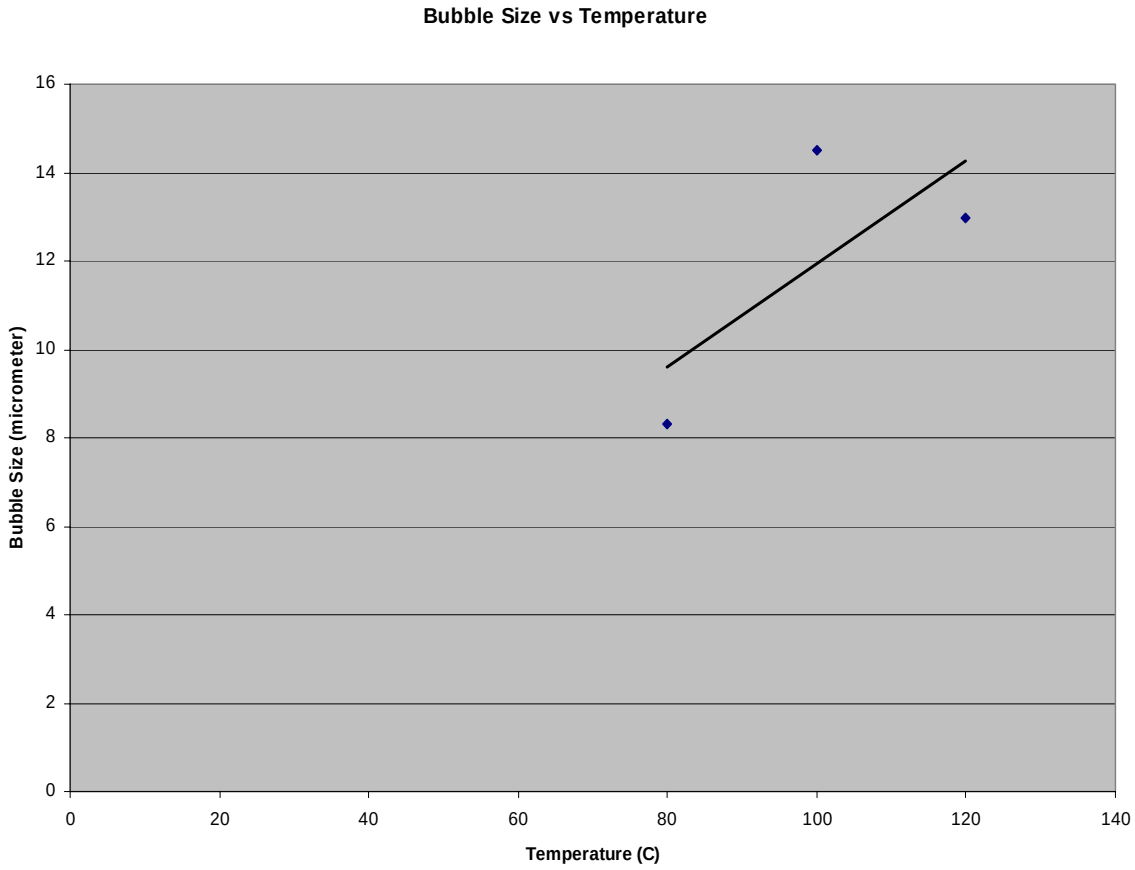

Figure 11: Plot showing the change in bubble size with changing foaming temperature for the 3% nanocomposite foams

The above figure shows the variation in the bubble size with changing foaming temperature. From the graph we can see that the linear trendline shows an increase in bubble size with increase in foaming temperature. Earlier, V. Kumar and J.E. Weller have shown that bubble size increases with increase in foaming temperature, (2). As described earlier, to come up with a convincing conclusion for the relationship between the foaming temperature and bubble size we need atleast 8-10 points due to the nature of the parameter varied i.e. temperature.

Other remarks during the experiment

Along with the above results relating the cell density and bubble size to the concentration as well as temperature, several other remarks were pointed out during the course of the experiment and during the analysis of the scanning electron micrographs. During the analysis of the scanning electron micrographs of the foamed samples it was found that some of the cells of the foamed samples were open cell foams whereas some were closed cell foams. There was no particular pattern observed. Controlling the operating conditions can help to generate open celled or closed celled foams. Open celled foams are the foams in which cells are connected to each other and the cell walls are dissipated. Only the cell struts and the ribs are left behind. Such foams are useful in several applications such as absorption, filtration, separation, insulation in vacuum environment, scaffolds for tissue engineering, etc. The closed cell foams are the ones in which cell walls are intact and each cell is enclosed by a thin wall. Closed celled foams are non-water absorbent and non-biodegradable and the cells in closed cell foams are not interconnected. They float and have great tensile strength. They are also impervious to

petroleum. They are used in a variety of light weight products and help in replacing the pure material. They are used in making thin walled products such as water bottles, sheets, pipes, films, gaskets, cushions, etc. Figure 12 below shows scanning electron micrographs of foamed samples with open and closed cell foams.

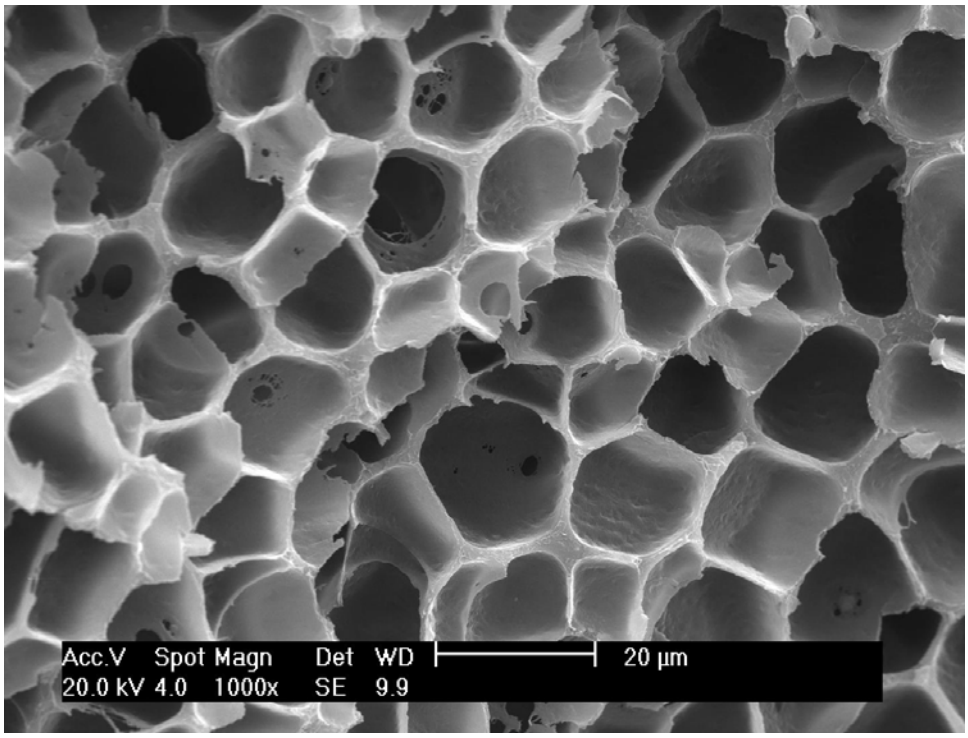

Figure 12: Scanning electron micrograph showing open cell and closed cell structure

The above picture shows both open as well as closed cell structures. The cells with continuous cell walls are closed cell foams and the cells with holes in the cell walls are open cell foams. Along with this it was also noticed that the foaming was uniform and homogeneous when images of different locations on the same cross section were observed. Figure 13 below compares two pictures to show that the foaming was uniform throughout the cross section.

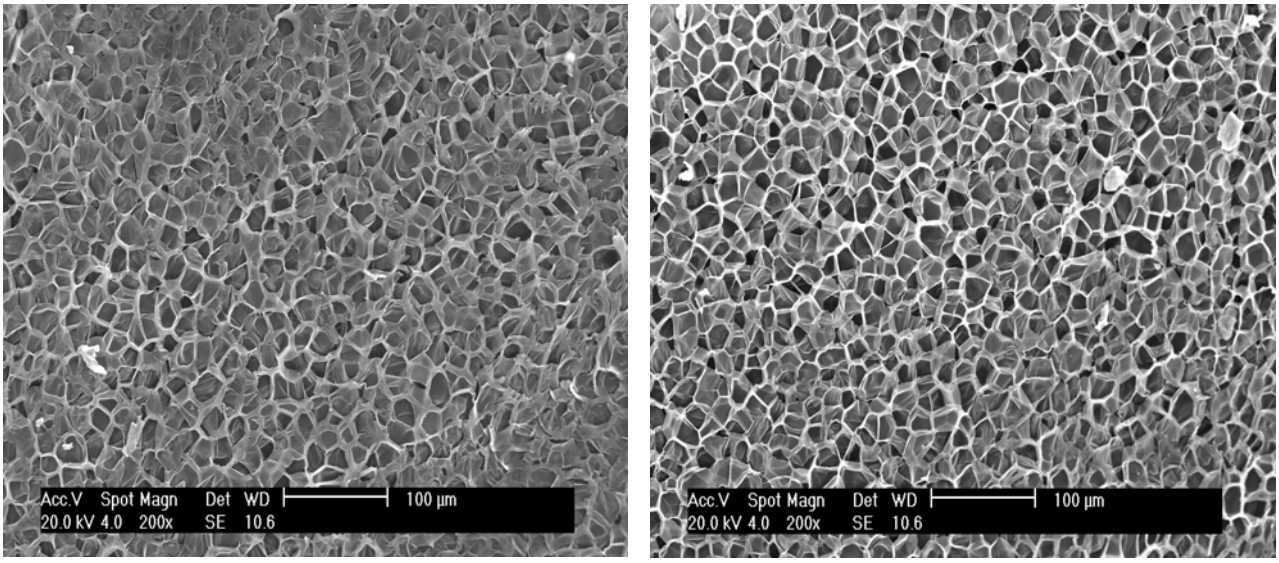

(a) (b)

Figure 13: (a) Image showing one half of a cross section cut using a sharp blade; (b) Image of the other half of the same cross section dissected in liquid nitrogen

The above images show that foaming was uniform throughout the cross section. Also, another interesting case was noticed when one of the trials with 1%, 0.1% and pure polystyrene loaded in the tube at 100° C were being foamed. After the end of the trial only 1% and 0.1% were foamed whereas the pure polymer that was places at the bottom of the tube did not foam and came out in the same way as it was introduced. These samples were discarded and the run was performed again when all the three samples loaded in the tube foamed. This might have to do with the fact that the glass transition temperature of polystyrene is close to 100° C. Some of the polymer samples underwent huge expansions in the foamed structures as compared to the others. Also, it is always advantageous to note down all the numbers during the course of foaming. For example, the initial and the final volume of the pump, the time for which foaming was performed

and the time for which the tube was cooled to allow expansion, the exact time it takes for the pressure to fall back to 0 psi from 2000 psi after the carbon dioxide is vented out, etc. All these could be useful in determining the behavior of the foams along with cell density and bubble size. For more convincing results it is always beneficial to have an average of several samples to indicate a particular number rather than just one sample at a specific temperature indicating a particular number. It would also be very helpful to repeat the trials atleast once more for precision and to achieve an accurate conclusion. For example, instead of loading three samples with different concentrations at 100° C introducing three pure polystyrene samples at 100° C would help to get an average cell density and bubble size. This could be checked by repeating the trial which would give a better number for cell density and bubble size. Due to lack of time, the trials could not be repeated during this work.

Conclusion:

We have presented a way to synthesize foams from polymer nanocomposites review along with a standard way to analyze the cell density and bubble size of intercalated nanocomposite polymer foams. The parameters affecting these properties of foams are also discussed. After synthesizing all the samples and their foams followed by the analysis of all the results it was found that the cell density increased with the increase in concentration and the bubble size decreased with the increase in concentration. The behavior of cell density with increasing concentration was in agreement with the literature. Also, the cell density decreased with the increase in foaming temperature and the bubble size increased with increase in foaming temperature. The behavior of cell density and bubble size was based only on three data points and hence is not convincing. More data is required to analyze the effect of foaming temperature on bubble size and density. In previous research, the bubble size is seen to increase with increase in temperature and the cell density is relatively independent of the foaming temperature. Both, open cell foams and closed cell foams were found in the scanning electron micrograph of the same cross section. Also, the foaming was uniform throughout the sample. Overall, foaming definitely improves the strength, toughness and other physical and mechanical properties of the polymer and also helps in saving the pure material. Polymer nanocomposite foaming is a very important area of research even today due to its wide applications in various industries.

Future Work:

I am a graduating senior at The Ohio State University and am currently enrolled in the BS/MS program in the Chemical Engineering Department. I am planning to pursue a PhD in Chemical Engineering after completing my BS/MS program. During my masters and PhD program I am planning to carry out more research in polymers. Out of all the research I am planning to perform in polymers, I think it would be interesting to test the effect of other parameters such as saturation pressure, foaming time, type of additive, etc on the cell density and the bubble size of the polymeric foams. Also, due to the complex behavior of temperature it would be challenging to perform more research to test the effect of temperature on the cell density and the bubble size of the foams. My focus will be to perform research with enough data points so that I can come up with a convincing conclusion for the effect of concentration and temperature as well as other parameters on cell density and bubble size. Also, the idea of performing multiple runs is appealing as it would give a more accurate value for every data entry which would help in deriving an appropriate conclusion. In addition to this, studying the wall characteristics of the polymeric foams would also be interesting.

Acknowledgments:

I would like to thank Dr. Koelling for all the time and support provided during the research. I would also like to thank Xiangmin Han and Jianhua Xu for all the help they provided to get the images using scanning electron microscope (SEM) along with The Ohio State University Medical Centre for allowing us to use the SEM facilities. Also, thanks to the graduate students Shunahshep and Sharath for the help they provided in getting me started with the research.

References:

1) Kumar, V. and Weller, J. E., 1993, 'A Process to Produce Microcellular PVC', Intern. Polymer Processing VIII, p. 73-80.
2) Kumar, V. and Weller J., (November 1994), 'Production of Microcellular Polycarbonate Using Carbon Dioxide for Bubble Nucleation', Journal of Engineering for Industry, Vol. 116, p. 413-420.
3) Colton, Jonathan S. and Suh, Nam P., 1987, 'Nucleation of Microcellular Foam: Theory and Practice', Polymer Engineering and Science, Mid-April, Vol. 27, No. 7, p. 500-503.
4) Zeng, Changchun and Lee, James L., 2001, 'Poly (methyl methacrylate) and Polystyrene/Clay Nanocomposites Prepared by in-Situ Polymerization', Macromolecules, Vol. 34, No. 12, p. 4098-4013.
5) Han, X., Zeng, C., Lee, James L., Koelling, Kurt W. and Tomasko, David L., June 2003, 'Extrusion of Polystyrene Nanocomposite Foams With Supercritical CO_2', Polymer Science and Engineering, Vol. 43, No. 6, p. 1261-1275.
6) Tomasko, David L., Han, X., Liu, Dehua and Gao, Weihong, 2003, 'Supercritical fluid applications in polymer nanocomposites', Current Opinion in Solid State and Materials Science 7, p. 407-412.
7) Tomasko, David L., Li, H., Han, X., Liu, D., Wingert, Maxwell J., Lee, James L. and Koelling, Kurt W., 2003, 'A Review of CO_2 Applications in the Processing of Polymers', Ind. Eng. Chem. Res., Vol. 42, No. 25, p. 6431-6456.